JOURNAL OF PROPULSION AND POWER
Vol. 10, No. 5, Sept.–Oct. 1994

Analysis of External Burning on Inclined Surfaces in Supersonic Flow

J. A. Schetz,* F. S. Billig,† and S. Favin‡
Johns Hopkins University, Laurel, Maryland 20723

An earlier analysis of a viscous mixing region with heat addition interacting with a supersonic external flow has been extended to include cases with a sloped wall beneath the viscous region. Also, cases with a supersonic to subsonic transition at the viscous throat have been studied for the first time. Limitations on the allowable heating value of the fuel that correspond to smooth subsonic to supersonic, or supersonic to subsonic transitions, are delineated and explained. The effects of wall slope at the throat and external Mach number on these limitations are shown. The results of calculations for representative cases show that it is possible to cancel base drag and even produce net thrust for cases with downward sloped walls if the initial Mach number in the viscous zone is supersonic prior to addition of heat. This corresponds to a supersonic to subsonic transition. For an initially subsonic flow, the results indicate pressures below the freestream static pressure throughout the flowfield. This means that only very limited drag from flameholders, such that the flow remains supersonic before heat addition, are advisable. Finally, some directions for future work are outlined.

Nomenclature

A = area of the viscous region
$\bar{A}$ = dimensionless area
a = slot height
c_p = specific heat
f_s = fuel/air weight ratio
h = height
h_f = heating value of fuel
K = constant in entrainment expressions
M = Mach number
$\dot{m}$ = mass flow in the viscous region
P = pressure
T_0 = total temperature
U = axial velocity
V = velocity in the viscous region
W = $\dot{m}/\dot{m}^*$, normalized mass flux
x = axial coordinate
$\bar{x}$ = x/A^*, normalized axial coordinate
β_w = wall angle
γ = ratio of specific heats
δ = boundary-layer thickness
θ = deflection angle
ρ = density

Subscripts
e = edge conditions
i = initial conditions in the injectant
0 = starting conditions in the mixing region
1 = undisturbed external stream conditions

Superscript
$*$ = viscous throat values

Presented as Paper 91-2390 at the AIAA/SAE/ASME/ASEE 27th Joint Propulsion Conference, Sacramento, CA, June 24–26, 1991; received Aug. 22, 1991; revision received Jan. 29, 1994; accepted for publication Feb. 2, 1994.

*Consultant, Applied Physics Laboratory; currently J. Byron Maupin Professor, Virginia Polytechnic Institute and State University, Blacksburg, VA 24061. Fellow AIAA.
†Chief Scientist, Applied Physics Laboratory, Aeronautics Department. Fellow AIAA.
‡Senior Programmer, Applied Physics Laboratory.

Introduction

THERE is a long history of interest in the use of heat release behind, adjacent to, or in front of supersonic projectiles and vehicles to provide propulsion or improve performance.[1–11] References 4 and 9 give reviews of the subject.

The analysis of such flows has proven challenging and interesting. In many cases, the appearance of a viscous throat with heat release plays a key role in the physics and mathematics of the flow.[7] Indeed, the study of the conditions at this viscous throat often serves to delineate clearly the conditions under which a presumed structure of the flow can or cannot actually exist. The analyst or experimentalist who neglects these important restrictions does so at his or her peril.

For design purposes, a relatively simple, and thus, computationally inexpensive analysis that retains at least approximate models of all the important physical, chemical, and mathematical features of the flows of interest is required. Analyses of that type for base burning cases were successfully developed in the 1970s.[7,8,10] The key features of those treatments were 1) the assumption of one-dimensional flow in the viscous region, 2) inviscid/viscous interaction with linearized supersonic theory in the external flow, 3) turbulence modeling through an expression for entrainment, and 4) a simple, one-step, diffusion-controlled model for heat release. A viscous throat appeared and played a central role in these analyses. Various extensions to other conditions have been developed.[11,12] These treatments predicted all the major qualitative and quantitative features of such flows that have been observed in experiments.

The present work involves extensions of the earlier analyses in two important ways. First, the occurrence of sloped surfaces that might occur along the nozzle of a large hypersonic, air breathing vehicle are now allowed. The interest here is in drag reduction at transonic and low supersonic Mach numbers. Second, attention is also focused on smooth supersonic to subsonic transitions through the viscous throat as well as the subsonic to supersonic transitions that occur in the classical base burning cases.

Analysis

The flowfield to be analyzed is shown schematically in Fig. 1. The complete flow will be treated with a modular approach. The upstream module (Module I) encompasses the combustor exit flow, the captured part of the external stream, any extra fuel injection, and a flameholder, if desired. Pressure mis-

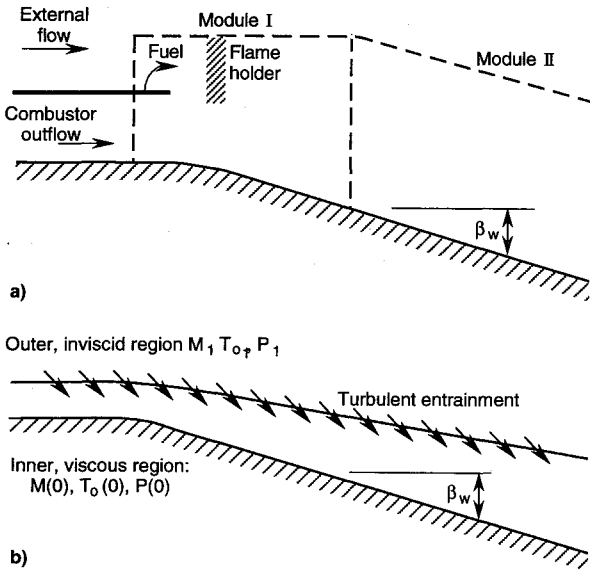

Fig. 1 Schematic illustration of the flowfield to be analyzed: a) complete flowfield and b) flowfield for Module II.

match between the combustor exit and the external flow is allowed. Module II encompasses the rest of the flow using the exit from Module I as inflow conditions. These conditions are taken as one-dimensional averages in the transverse direction.

A schematic diagram of the flowfield model adopted for Module II is shown in Fig. 1b. The analysis of Module II will be discussed first. Also, some problems might not have an actual Module I if the upstream arrangement of interest is simpler than that shown in Fig. 1a. The external stream is presumed supersonic, and the inner stream may be initially either subsonic or supersonic.

Downstream of the initial station for Module II, the inner flow is treated as a one-dimensional flow whose change in properties with x represents a suitable average of the real fluid properties with mass entrainment from the outer stream. The equations developed in Ref. 13 are used to define the Mach number change in the inner stream, viz.,

$$\frac{dM^2}{M^2} = -2\frac{1+[(\gamma-1)/2]M^2}{1-M^2}\left[\frac{dA}{A} - \frac{1+\gamma M^2}{2}\frac{dT_0}{T_0} + \gamma M^2\frac{U_e}{V}\frac{d\dot{m}}{\dot{m}} - (1+\gamma M^2)\frac{d\dot{m}}{\dot{m}}\right] \tag{1}$$

Here, we have assumed that the ratio of specific heats and the molecular weight of the fluid remain constant. This assumption can be relaxed with only a small penalty in added complexity.

The term $(U_e/V)(d\dot{m}/\dot{m})$ represents the momentum contribution of freestream fluid that is entrained into the mixing zone. Taking $U_e = U_1$, the freestream velocity upstream, and employing the required identities results in

$$\frac{U_e}{V}\frac{d\dot{m}}{\dot{m}} = \frac{M_1}{M}\sqrt{\frac{(T_{01}/T_0)\{1+[(\gamma-1)/2]M^2\}}{1+[(\gamma-1)/2]M_1^2}} \tag{2}$$

Consider now the stagnation temperature change term dT_0/T_0. When the fluid in the inner stream is initially fuel rich, it can react with the freestream fluid mixing downstream and produce a T_0 change by two effects. First, freestream fluid entrained into the mixing zone carries with it thermal energy based upon T_{01}. This can either heat or cool the mixing zone, depending on the relative magnitudes of T_{01} and T_0. Second, heat can be released in proportion to the amount of freestream fluid entrained into the fuel-rich mixing zone and the heating value of the fuel. If we take a simple, constant heating value model of the reaction, these two effects can be represented as

$$\frac{dT_0}{T_0} = \left[\frac{T_{01}-T_0}{T_0} + \frac{\bar{h}_f f_s}{c_p T_0}\right]\frac{d\dot{m}}{\dot{m}} \tag{3}$$

This simple expression carries a profound message in that unless the second term in the bracket is larger than the first, there will be net cooling even though there is heat release. That situation can easily occur if the inner stream is initially hot and contains a fuel with a low heating value.

It remains now to model the turbulent transport processes which appear here as entrainment, i.e., $d\dot{m}/dx$. Crocco and Lees[14] used, principally for boundary-layer-type flows, simply

$$\frac{d\dot{m}}{dx} = K\rho_e U_e \tag{4}$$

where K is a constant $\approx 0.01-0.03$. The higher values were for separated or separating flows. For the present problem, it appears necessary to extend this relation to account for the extremely small amount of entrainment for the situation in which $\rho_e U_e = \rho U$, i.e., the mass flux in the freestream and the inner viscous zone are the same. Most successful eddy viscosity models predict a zero Reynolds stress for the same condition. Thus, we have employed

$$\frac{d\dot{m}}{dx} = K\rho_1 U_1\left|1-\frac{\rho U}{\rho_1 U_1}\right| \tag{5}$$

Extensive comparisons of predictions and experiment have led us to adopt a "universal" value $K = 0.02$. Also, the mass flow rate $\dot{m}$ has been nondimensionalized by the value at the viscous throat, $(\dot{m})^*$, i.e.,

$$W = \frac{\dot{m}}{\dot{m}^*} = \frac{\rho UA}{(\rho UA)^*} = \frac{(\rho U/\rho_1 U_1)\bar{A}}{(\rho U/\rho_1 U_1)^*} \tag{6}$$

where $\bar{A} \equiv A/A^*$. With this and Eq. (5), we get

$$\frac{\bar{A}}{W}\frac{dW}{d\bar{x}} = K\left[\frac{1}{\rho U/\rho_1 U_1}\right] - 1 \tag{7}$$

which can be easily related to the $d\dot{m}/\dot{m}$ terms in Eq. (1).

Finally, the pressure variation in the inner flow, which must be balanced with that in the outer flow at the same x, is given by

$$\frac{1}{P}\frac{dP}{dx} = \frac{1}{\dot{m}}\frac{d\dot{m}}{dx} - \frac{1}{A}\frac{dA}{dx} - \frac{1}{2M^2}\frac{dM^2}{dx}\left\{\frac{1+(\gamma-1)M^2}{1+[(\gamma-1)/2]M^2}\right\} + \frac{1}{2T_0}\frac{dT_0}{dx} \tag{8}$$

The outer, inviscid, supersonic flow is assumed to be adequately described by the linearized supersonic theory:

$$\frac{dP}{P} = \frac{\gamma M_1^2}{\sqrt{M_1^2-1}}d\theta \tag{9}$$

In order to determine θ, one can write

$$\frac{d\dot{m}}{dx} = \rho_1 U_1\left(\frac{dA}{dx} - \theta + \beta_w\right) \tag{10}$$

Now using Eq. (5)

$$\theta = \frac{dA}{dx} - K\left(1-\frac{\rho U}{\rho_1 U_1}\right) + \beta_w \tag{11}$$

Thus

$$\frac{1}{P}\frac{dP}{dx} = \frac{\gamma M_1^2}{\sqrt{M_1^2 - 1}}\frac{d}{dx}\left[\frac{dA}{dx} - K\left(1 - \frac{\rho U}{\rho_1 U_1}\right) + \beta_w\right] \quad (12)$$

Compatibility Condition

Matching the pressure in the inner and outer regions, i.e., Eqs. (8) and (12), gives

$$\frac{\gamma M_1^2}{\sqrt{M_1^2 - 1}}\frac{d}{d\bar{x}}\left[\frac{d\bar{A}}{d\bar{x}} - K\left(1 - \frac{\rho U}{\rho_1 U_1}\right) + \beta_w\right] = \frac{1}{W}\frac{dW}{d\bar{x}} - \frac{1}{\bar{A}}\frac{d\bar{A}}{d\bar{x}} + \frac{1}{2T_0}\frac{dT_0}{d\bar{x}} - \frac{1}{2M^2}\frac{dM^2}{d\bar{x}}\left[\frac{1 + (\gamma - 1)M^2}{1 + [(\gamma - 1)/2]M^2}\right] \quad (13)$$

This can be integrated to yield

$$\frac{d\bar{A}}{d\bar{x}} = \left(\frac{d\bar{A}}{d\bar{x}}\right)^* + K\left[\left(\frac{\rho U}{\rho_1 U_1}\right)^* - \left(\frac{\rho U}{\rho_1 U_1}\right)\right] - \frac{\sqrt{M_1^2 - 1}}{\gamma M_1^2} \times \int\left[\left(\frac{M\bar{A}}{W}\right)\frac{\sqrt{[2/(\gamma + 1)]\{1 + [(\gamma - 1)/2]M^2\}}}{\sqrt{T_0/T_0^*}}\right] - (\beta_w - \beta_w^*) \quad (14)$$

The solution would be straightforward except for the occurrence of the $(1 - M^2)$ term in the denominator of Eq. (1). This singularity is more than just a nuisance, however, since it is the key to setting the initial pressure for a given set of conditions. Only one value of the initial pressure for a given problem will allow a smooth passage through the viscous throat. To determine the starting conditions, it is necessary to apply L'Hospital's Rule to Eq. (1). Leaving out the requisite derivation, the result may be written schematically

$$\left(\frac{dM^2}{d\bar{x}}\right)^* = \frac{-b + \sqrt{b^2 - 4c}}{2} \quad (15)$$

where

$$b = \frac{\sqrt{M_1^2 - 1}}{M_1^2} + \frac{\gamma(\gamma + 1)}{2}\left(\frac{1}{T_0}\frac{dT_0}{d\bar{x}}\right)^* - K\exp\left\{\frac{-\gamma M_1^2}{\sqrt{M_1^2 - 1}}\left(\frac{d\bar{A}}{d\bar{x}}\right)^* + \beta_w - K\left[1 - \frac{(\rho U)^*}{\rho_1 U_1}\right]\right\} \times \left\{\gamma^2 M_1^2 - \frac{(\gamma + 1)M_1\sqrt{1 + [(\gamma - 1)/2]M_1^2}}{\sqrt{[(\gamma + 1)/2](T_{01}/T_0^*)}} \times \left(\frac{1}{\gamma + 1} - 2\gamma\right)\right\} + \frac{K\gamma M_1\sqrt{[(\gamma + 1)/2](T_{01}/T_0^*)}}{\sqrt{1 + [(\gamma - 1)/2]M_1^2}} - K\gamma(\gamma + 1) \quad (16)$$

$$c = \frac{(\gamma + 1)\sqrt{M_1^2 - 1}}{\gamma M_1^2}\left[\left(\frac{d\bar{A}}{d\bar{x}}\right)^* - \left(\frac{1}{2T_0}\frac{dT_0}{d\bar{x}}\right)^* - \left(\frac{dW}{d\bar{x}}\right)^*\right] + \left(\frac{\gamma + 1}{2}\right)^2\left[\left(\frac{d\bar{A}}{d\bar{x}}\right)^*\left(\frac{1}{T_0}\frac{dT_0}{d\bar{x}}\right)^* + \frac{d}{d\bar{x}}\left(\frac{1}{T_0}\frac{dT_0}{d\bar{x}}\right)^*\right] - K\left(\frac{\gamma + 1}{2}\right)\left(2\left\{\gamma M_1^2 - \frac{(\gamma + 1)M_1\sqrt{1 + [(\gamma - 1)/2]M_1^2}}{\sqrt{[(\gamma + 1)/2](T_{01}/T_0^*)}}\right\}\left[\left(\frac{d\bar{A}}{d\bar{x}}\right)^* - \left(\frac{1}{2T_0}\frac{dT_0}{d\bar{x}}\right)^* - \left(\frac{dW}{d\bar{x}}\right)^*\right] + \frac{M_1\sqrt{1 + [(\gamma - 1)/2]M_1^2}}{\sqrt{[(\gamma + 1)/2](T_{01}/T_0^*)}}\left(\frac{1}{T_0}\frac{dT_0}{d\bar{x}}\right)^*\right) \Bigg/ \exp\left\{\frac{\gamma M_1^2}{\sqrt{M_1^2 - 1}}\left[\left(\frac{d\bar{A}}{d\bar{x}}\right)^* - K\left(1 - \frac{\rho U}{\rho_1 U_1}\right)^* + \beta_w^*\right]\right\} + K\gamma\left(\frac{\gamma + 1}{2}\right)\left(\frac{1}{T_0}\frac{dT_0}{d\bar{x}}\right)^*\frac{M_1\sqrt{[(\gamma + 1)/2](T_{01}/T_0^*)}}{\sqrt{1 + [(\gamma - 1)/2]M_1^2}} \quad (17)$$

Mathematical Overview and Initial Conditions

The mathematical formulation is contained in Eqs. (1) [with (2)], (3), (7), and (14). They were all rewritten in terms of nondimensional variables and programmed for solution by means of the Adams-Moulton or Gear (if the system is "stiff") method. The well-tested routine DIVPAG from IMSL was used. The system is often stiff. As in Ref. (14), it is more convenient to begin the analysis at the viscous throat with assumed conditions and proceed upstream seeking a matching of the initial conditions through successive iterations, than to guess the initial conditions and seek to pass through the saddle point singularity. Moreover, each solution generated in the iterative procedure corresponds to a valid solution for a set of initial conditions and thus provides a library of solutions that can be used for parametric studies, other particular problems, etc. Once the desired upstream match is found, the solution can also be found downstream of the viscous throat using the same numerical methods.

The starting conditions in the mathematical analysis are, therefore, the viscous throat conditions, viz.

$$M = \bar{A} = W = (T_0/T_0^*) = 1$$

The (+) sign before the quadratic in Eq. (15) is the appropriate choice on the basis of the second law. It is important to note here that we must have $c > 0$ in order to have a passage from a subsonic to a supersonic flow at the viscous throat. For a smooth supersonic to subsonic passage, $c < 0$. This has a significant effect on the solution, as will be seen later.

The analysis of Module I is relatively simple from a mathematical point of view. We apply conservation of mass, momentum, and energy in an integral sense with one-dimensional averages for the inflow and outflow streams. Entrainment from the external flow is modeled as for Module II. The flameholder is represented by a given area and drag coefficient. A simple, one-step model is again used for heat release. This all results in a system of algebraic equations with the outflow conditions and the length of Module I as the unknowns. Solutions for a given set of conditions are sought for a range of values of the output pressure ratio P_2/P_1. This produces a trace of P_2/P_1 vs $\rho_2 U_2/\rho_1 U_1$. The correct solution is found by intersection with the solution of Module II proceeding upstream from the viscous throat. The process will be clarified and illustrated in the Results section below. This produces a complete, composite solution for the whole flow.

Results

We begin with results from Module II standing alone. This is for clarity and to illustrate some important points. Also, some flow problems may not require a Module I at all. That might happen when there is no flameholder or extra fuel injection and the pressures are matched at the end of the combustor.

The reader can refer to Refs. 7, 8, and 10–12 for extensive comparisons of the predictions of the basic analysis with experiment over a wide range of conditions. These comparisons serve to demonstrate the adequacy of the various assumptions and modeling choices made including, in particular, turbulence modeling through an entrainment law and the universal value $K = 0.02$. However, all of the cases considered in those works did not have sloped walls or supersonic to subsonic passage through a viscous throat.

There is one relevant experiment in the literature with sloped walls.[15] However, that experiment is supersonic ($M_j = 1.98$) slot injection into a supersonic ($M_1 = 2.85$) stream with downstream wedges of various positive angles, such that there is no viscous throat in the flowfield. Also, the larger wedge angles produced large separation zones that cannot be treated by the present type of analysis. Nonetheless, it is useful to make comparisons of the predictions of the current type of analysis[12] with the limited data available for a 5-deg wedge case. The only data available is $P(x)$ before the wedge and schlieren photographs. A comparison of the predicted and measured $P(x)$ is shown in Fig. 2. Also indicated is the pressure rise on a 5-deg wedge in a uniform $M_1 = 2.85$ flow for reference. One can expect the current flow to achieve that value far downstream. This is a complex case, since $P_j/P_1 < 1$ leading to a wave structure in the inner stream. In spite of all this, the comparison can be judged as reasonable. It is also possible to measure $A(x)$ from the schlieren photographs and compare with the predictions. The comparison is good but rather uninteresting, since the initial pressure adjustment, turbulent entrainment, and the wedge turn all combine to produce an $A(x)$ that varies little in the range of the experimental observations. We take these results as a limited justification of our treatment of the influence of a sloped wall in the flow.

We mentioned earlier that the sign of "c" in Eqs. (15) and (17) is very important in determining the types of flowfields that can exist with smooth passages through the viscous throat. In classical base flow problems with injection and burning, the initial conditions in the inner stream are generally low subsonic with a supersonic external stream. In such cases, the passage through the viscous throat is from subsonic to supersonic conditions. We found that this required $c > 0$ (Ref. 7), and that led to surprisingly tight restrictions on the combination of flow conditions and parameters allowed. In particular, only fuels with a relatively low net heating value could be used. Here, we wish to consider supersonic to subsonic passage through a viscous throat with heat release also. A

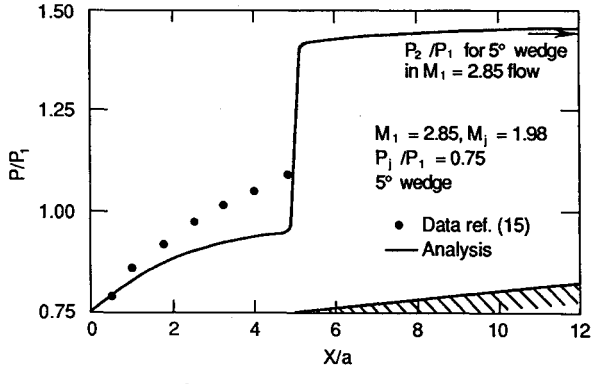

Fig. 2 Comparison of prediction and experiment for wall pressure distribution for slot injection over a ramp.

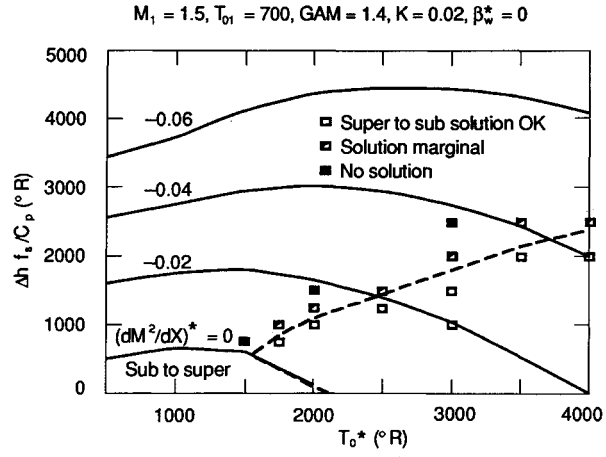

Fig. 3 Limitations on allowable heat release implied by conditions at the viscous throat.

typical map of the allowable conditions is shown on Fig. 3 for a set of representative flow conditions. The ordinate is the heating value of the fuel, and the abscissa is the total temperature at the viscous throat. The first boundary of interest is the curve marked $(dM^2/dx)^* = 0$. The region below that curve is for subsonic to supersonic passages through the viscous throat, and the region above is for supersonic to subsonic passages. Obviously, more heat release (higher $\bar{h}_f f_s/c_p$ values) is required to reduce the Mach number counteracting the acceleration effects of shear from the external stream. However, we have found an interesting and important second boundary denoted here by the dashed curve going up to the right. Above this curve, the numerical solutions could not be made to move smoothly upstream from the viscous throat. Various attempts with very small step sizes, tight tolerances, etc., failed to resolve this problem. The solution always seemed to want to jump to another branch which had increasing Mach number putting it back through the viscous throat the other way. One finds that this boundary corresponds to cases with dT_0/T_0 approaching zero from below. This is similar to the "entropy limit" solutions, but with the limit approaching from above, found appropriate in the analysis of Ref. 16. This matter needs further study, but we believe that the limitations implied are real.

The map such as shown in Fig. 3 is affected by both external stream Mach number and the presence of wall slope at the viscous throat. Increasing the external stream Mach number moves the boundaries up. For example, with $M_1 = 2.0$ and $T_{01} = 900$°R, the $(dM^2/dx)^* = 0$ curve intersects the ordinate at just over 1000 (compared to 500 at $M_1 = 1.5$) and the abscissa at about 3600 (compared to 2100 at $M_1 = 1.5$). The dashed curve also moves up to intersect the $T_0^* = 4000$ line at about 2800 (compared to about 2400 at $M_1 = 1.5$). For a given M_1, the effect of negative wall angles at the viscous throat is to move the boundaries up somewhat.

Subsonic to Supersonic Transition

Consider first cases with a subsonic to supersonic passage through the viscous throat. The usual base flow cases fall in this category. Here, we shall be interested in showing the effects of a sloped wall at the viscous throat. This kind of case will arise in the external burning application whenever even a modest loss mechanism is present, e.g., a low drag flameholder.

For illustrative purposes, a series of cases with $M_1 = 2.0$, $T_{01} = 900$°R and $T_0^* = 1800$°R were chosen. A heating value of the fuel of $\bar{h}_f f_s/c_p = 1100$°R was selected, since that is near the maximum allowed for a subsonic to supersonic passage through the viscous throat at these conditions. The results of three cases are shown in Figs. 4a–4c. The difference between these cases is the magnitude of the slope of the wall. In Fig. 4a, the wall is straight, i.e., $\beta_w^* \equiv 0$. It is most instructive to

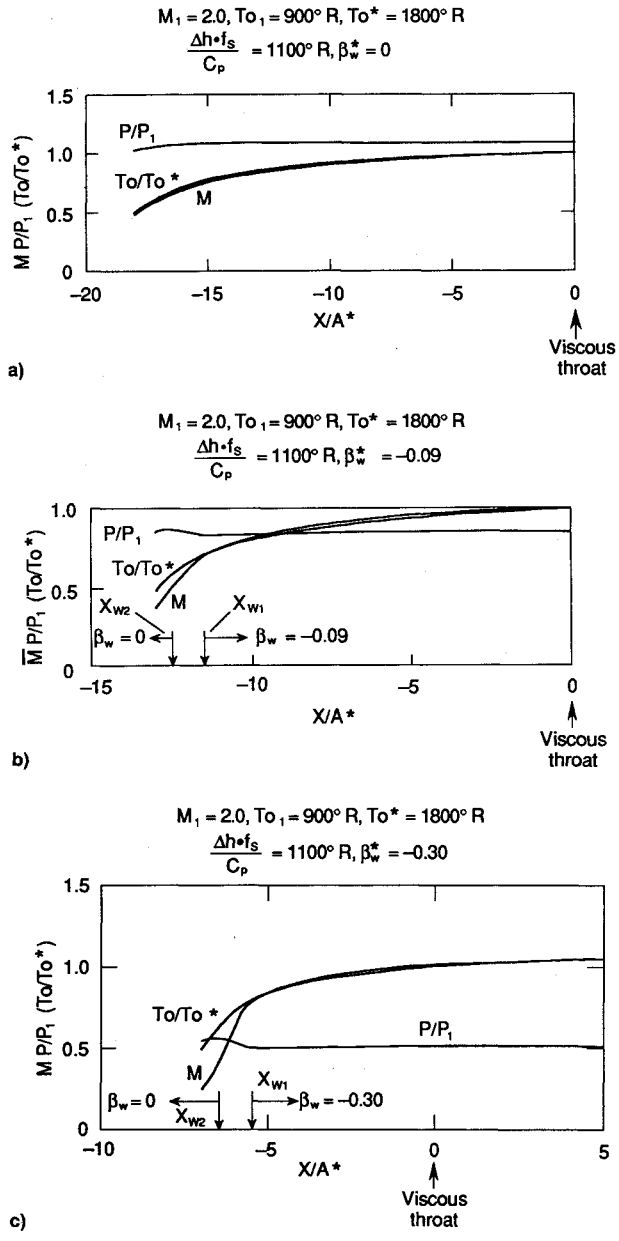

Fig. 4 Predicted flowfield upstream of the viscous throat for subsonic initial flow in the viscous region with heat release: a) straight wall ($\beta_w^* \equiv 0$), b) sloped wall ($\beta_w^* = -0.09$), and c) sloped wall ($\beta_w^* = -0.30$) with downstream prediction.

view the results as starting at the viscous throat ($x/A^* = 0$) and then proceeding upstream ($x/A^* < 0$). Note that the pressure at the viscous throat is slightly above P_1, and that it decays slightly at the assumed upstream "initial" conditions $T_0 = T_{01}(T_0/T_0^* = 0.5)$. The total temperature increases steadily and smoothly from that point downstream to the viscous throat. Likewise, the Mach number increases steadily from an initial value of about 0.5 at that point up to a unity value at the throat.

The case in Fig. 4b is different by the presence of a downward sloped wall at the viscous throat ($\beta_w^* = -0.09$). Proceeding upstream, the wall slope is decreased starting at x_{w1} to a value of 0 at x_{w2}. The first result is to shorten the flowfield in dimensionless terms (x/A^*). The second obvious result is a decrease in pressure at the viscous throat to a value of about $0.86P_1$. With some slight variations, it ends up about at the same value at the upstream initial conditions where $T_0 = T_{01}$. The Mach number at that point for this case is about 0.38. The behavior of the pressure should not be surprising, since, without heat release, there would be a substantial expansion over the sloped wall. If the approach flow to the ramp were uniform at the external stream value of $M_1 = 2.0$ and there were no heat release, the pressure on the sloped wall would drop to $0.74P_1$.

In Fig. 4c, the results for a wall with a greater downward slope ($\beta_w^* = -0.30$) are given. The flowfield is foreshortened more in dimensionless terms. The pressure at the viscous throat is reduced to approximately $0.51P_1$, and it increases slightly to $0.55P_1$ at the upstream initial point. The Mach number at that point is reduced to about 0.25. Again, with no heat release, one could expect the pressure to reduce to $0.34P_1$ on the ramp. Also shown on Fig. 4c are the results of calculations downstream of the viscous throat ($x/A^* > 0$). Nothing startling happens. The Mach number (now > 1.0) and the total temperature contrive to increase smoothly and rather slowly. The pressure remains nearly constant.

The behavior of the total temperature variation for these typical cases can be understood more closely by referring to Eq. (3). At the "initial," upstream station, $T_0 = T_{01}$, so that the first term in the brackets is 0, and the second term is positive and relatively large. The value of T_0 in the denominator is at its minimum. Proceeding downstream, $T_0 > T_{01}$, so that the first term becomes negative and the second term becomes smaller. This results in a rapid initial increase in T_0, followed by a steadily decreasing rate of increase downstream.

Supersonic to Subsonic Transition

A case of this type can be constructed by taking a case such as in Fig. 4c and presuming a fuel with a higher heating value. Looking at Fig. 3, one can see that a higher heating value can move the problem into a regime where $(dM^2/dx)^* < 0$. We have selected $\bar{h}_f f_s/c_p = 1500°R$ and a higher total temperature at the viscous throat of $T_0^* = 2700°R$ to go with it. These conditions are just below the dashed boundary in a $M_1 = 2.0$ plot corresponding to Fig. 3.

The predicted flowfield results are plotted in Fig. 5. Several important differences are immediately apparent compared to the corresponding case in Fig. 4c (same M_1, T_{01}, β_w^*). First, the Mach number decreases rather rapidly through the throat. One can postulate an upstream initial condition where $M = M_1 = 2.0$. Second, T_0 now slowly decreases through the whole flow. Third, the pressure at the throat is $0.71P_1$, and it decreases to $0.17P_1$ at the initial station. Perhaps more importantly, we see $P > P_1$ after some distance downstream of the throat. Values approaching $1.5P_1$ are clearly possible. This is a very promising result, since it implies that net thrust may indeed be achievable under such conditions. How this pressure field is produced can be better understood by examining the viscous area distribution $(A/A^*)(x)$. At the upstream boundary, the area change is sloped down corresponding to a low pressure. It reaches a minimum (not at the viscous throat) and then increases. This increase is rather rapid on

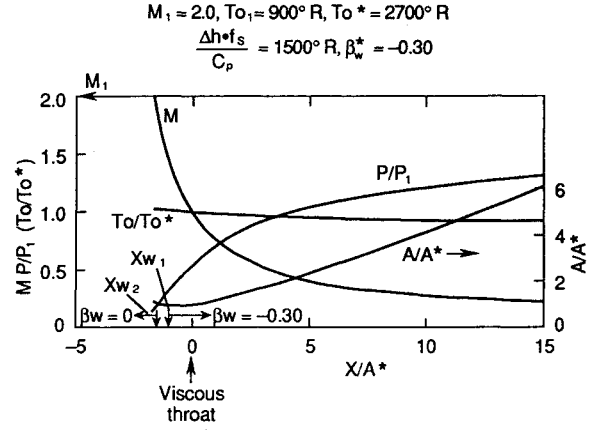

Fig. 5 Predicted flowfield for supersonic initial flow in the viscous region with heat over a sloped wall ($\beta_w^* = -0.30$).

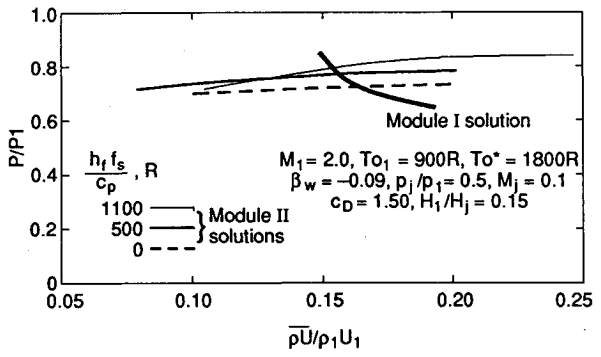

Fig. 6 Composite solution for a representative case.

the subsonic side, and this leads to an increasing pressure by interaction with the external supersonic stream.

Joining with Upstream Module Solutions

Consider a case as in Fig. 4b as an illustrative example. The additional parameters necessary to describe the flow in Module I are: P_j/P_1, M_j, C_D, H_1 (the height of the flameholder)/H_j, and T_{0j}. Calculations were run with values of 0.50, 0.10, 1.50, 0.15, and 900°R. The trace of possible solutions is shown as the solid line in Fig. 6. The trace of the solution of Module II from the viscous throat upstream for the case in Fig. 4b is shown as a thin solid line on Fig. 6, and the unique solution to this whole problem is the intersection of the two traces. One can then investigate the effect of the heat release parameter, as an example, on the solution. A Module II solution trace with $\bar{h}_f f_s/c_p$ reduced to 500°R is plotted as a medium solid line in Fig. 6, and a solution with this parameter reduced all the way to 0.0 is plotted as a short-dash line in Fig. 6. Clearly, reducing the heat release reduces the static pressure on the ramp.

Conclusions

Analysis of a viscous mixing region with heat addition interacting with an external supersonic flow has been extended to cases with a sloped wall beneath the viscous region. Also, cases with a smooth supersonic to subsonic passage through the viscous throat have been considered in detail for the first time.

An essential feature of such flows is the behavior of the solution at the viscous throat. Various limitations exist on the types of flows that are allowed for a given combination of conditions and parameters. For example, if a flow that is initially subsonic in the viscous zone is to pass smoothly into the supersonic regime through the viscous throat, the heating value of the fuel is bounded from above for a given set of M_1, T_{01}, and T_0^*. Higher heating values correspond to a supersonic to subsonic passage. For cases with a supersonic to subsonic passage, another boundary was empirically found that limits the magnitude of the heating value. It corresponds to $(dT_0/T_0) < 0$ and is analogous to the entropy limit solutions for flow in ducts with heat addition found in Ref. 16. This means that the net heating values allowed are restricted to a rather narrow band for supersonic to subsonic transitions. If the wall is sloped down at the viscous throat, all these boundaries move up, corresponding to higher allowable net heating values. Increasing M_1 also moves the boundaries up, but only slightly.

The existence and meaning of these limitations may seem puzzling and indeed troubling. They do, however, really exist. For example, analyses of the type developed here correctly predict the limitations on base pressure behind a blunt-tailed body in a supersonic flow with base injection, with or without burning. For a given mass flux of injectant at subsonic speeds through the base, one cannot independently set the pressure at the injection point. Conditions at the downstream viscous throat with a subsonic to supersonic passage restrict the upstream base injection pressure to a unique value. It is worth noting here that no inviscid solution procedure, no matter how sophisticated, can correctly predict such a flow.

The result of all of this is important from a practical point of view. Earlier calculations have shown that it is difficult to get $P > P_1$ by more than a few percent with base burning using subsonic injection (on the average over the base area). Extensive experimental studies have confirmed that result. The limitations are a direct result of conditions at the viscous throat. The present calculations show that sloping the wall down at the viscous throat with subsonic initial conditions shifts the level of the static pressure down throughout the flow. A typical case with a −17-deg wall slope at $M_1 = 2.0$ has a static pressure of $0.51P_1$ at the viscous throat, $0.55P_1$ at the initial station, and $0.50P_1$ far downstream. However, if the initial upstream condition in the viscous region is supersonic, the pressure is low at the viscous throat ($0.71P_1$) and very low at the initial station ($0.17P_1$), but it increases to values $P \approx 1.5P_1$ far downstream. That means that cancellation of base drag and even production of net thrust is possible on sloped walls for the initially supersonic condition, but not if the flow in the viscous region is initially subsonic. In turn, that severely restricts the use of flameholders, since, at low M_1, even a modest drag from flameholders will lead to subsonic flow ahead of the heat release zone.

Some discussion of what is likely to happen if the limits on fuel heating value discussed in this article are violated is appropriate. The first useful clue can be found in previous related work for flow in ducts with heat addition (see Ref. 13, Chap. 7). There, it is shown that if the ΔT_0 is too great for a given initial supersonic Mach number, a large scale rearrangement of the upstream flow results such that a shock system occurs in the supersonic nozzle leading to a reduced supersonic value of the initial Mach number approaching the heat release zone. For very large ΔT_0, the flow becomes subsonic everywhere. If the initial flow is subsonic and ΔT_0 is increased above the maximum allowed, the upstream flow is again forced to adjust now by reducing the flow rate and the initial Mach number. These phenomena have all been verified by experiment.

For the present flow problem, we believe that a high heating value (too large ΔT_0) will result in large scale upstream adjustments in the viscous region, and also likely the external flow, in the form of shocks. A shock in the external flow, e.g., changes the pressure and the Mach number, etc., and this leads to changes in the viscid/inviscid interaction and entrainment which can influence the actual ΔT_0 that results. This allows the flow to adjust to allowable conditions as in the duct case. A second useful clue can be found in the observations of flows in ejectors. For certain combinations of mainstream and injected stream conditions, large recirculation regions are found to occur. Some workers attribute this to a need to satisfy a certain entrainment rate into the mixing zone by recirculating downstream fluid. Indeed, the flows in ducts with heating just discussed usually involve recirculation zones when upstream adjustments are produced. One can then presume that embedded recirculation zones are likely to occur in the present flow problem under those conditions. Recirculation of downstream fluid changes the apparent approach values of the total temperature and the mixture ratio in the viscous zone for a given entrainment rate. That can change the effective heating value as needed.

The current type of analysis cannot predict the details of the kind of phenomena discussed above. It can predict the boundaries where some type of large scale rearrangement of the flowfield will occur. One will have to look to careful experimental studies to show the form of the rearrangements that will occur in this flow problem. It should also be possible for comprehensive CFD analysis to be used to study such issues.

References

[1]Baker, W. T., Davis, T., and Matthews, S. E., "Reduction of Drag of a Projectile in a Supersonic Stream by the Combustion of Hydrogen in the Turbulent Wake," Johns Hopkins Univ., Applied Physics Lab., Rept. CM-637, Silver Spring, MD, 1951.

[2]Townend, L. H., and Reid, J., "Some Effects of Stable Combustion in Wakes Formed in a Supersonic Stream," *Supersonic Flows, Chemical Processes, and Radiative Transfer*, edited by D. B. Olfe and V. Zakkay, Pergamon, New York, 1964.

[3]Billig, F. S., "Supersonic Combustion at Storable Liquid Fuels in Mach 3.0 to 5.0 Air Streams," Xth Symposium (International) on Combustion, The Combustion Inst., Pittsburgh, PA, 1965.

[4]Billig, F. S., "External Burning in Supersonic Streams," *Proceedings of the XVIIIth International Astronautical Congress*, Pergamon, London, 1969, pp. 23–54.

[5]Smithey, W., and Fuhs, A. E., "Base Pressure Calculations with External Burning," *Aerodynamics of Base Combustion*, edited by S. N. B. Murthy, Vol. 40, Progress in Astronautics and Aeronautics, AIAA, New York, 1976, pp. 407–424.

[6]Strahle, W. C., Mehta, G., and Hubbartt, J. E., "Progress on a Base Flow Model for External Burning Propulsion," *Aerodynamics of Base Combustion*, edited by S. N. B. Murthy, Vol. 40, Progress in Astronautics and Aeronautics, AIAA, New York, 1976, pp. 339–348.

[7]Schetz, J. A., and Billig, F. S., "Approximate Analysis of Base Burning in Supersonic Flow," *Aerodynamics of Base Combustion*, edited by S. N. B. Murthy, Vol. 40, Progress in Astronautics and Aeronautics, AIAA, New York, 1976, pp. 385–406.

[8]Schetz, J. A., and Billig, F. S., "Simplified Analysis of Supersonic Base Flows Including Injection and Combustion," *AIAA Journal*, Vol. 14, No. 1, 1976, pp. 7, 8.

[9]Murthy, S. N. B., and Osborn, J. R., "Base Flow Phenomena with and Without Injection," *Aerodynamics of Base Combustion*, edited by S. N. B. Murthy, Vol. 40, Progress in Astronautics and Aeronautics, AIAA, New York, 1976, pp. 7–210.

[10]Schetz, J. A., Billig, F. S., and Favin, S., "Approximate Analysis of Axisymmetric Supersonic Base Flows with Injection," *AIAA Journal*, Vol. 18, No. 8, 1980, pp. 867, 868.

[11]Schetz, J. A., Billig, F. S., and Favin, S., "Analysis of Base Drag Reduction by Base and/or External Burning," *AIAA Journal*, Vol. 19, No. 9, 1981, pp. 1145–1150.

[12]Schetz, J. A., Billig, F. S., and Favin, S., "Analysis of Slot Injection in Hypersonic Flow," *Journal of Propulsion and Power*, Vol. 7, No. 1, 1991, pp. 115–122.

[13]Shapiro, A. H., *The Dynamics and Thermodynamics of Compressible Fluid Flow*, Ronald Press, New York, 1953.

[14]Crocco, L., and Lees, L., "A Mixing Theory for the Interaction Between Dissipative Flows and Nearly Isentropic Streams," *Journal of the Aeronautical Sciences*, Vol. 19, No. 10, 1952, pp. 649–676.

[15]Gilreath, H. E., "An Investigation of Gaseous Tangential Injection in Supersonic Flow," Ph.D. Dissertation, Univ. of Maryland, College Park, MD, 1968.

[16]Billig, F. S., and Dugger, G. L., "The Interaction of Shock Waves and Heat Addition on the Design of Supersonic Combustors," *XIIth Symposium (International) on Combustion*, The Combustion Inst., Pittsburgh, PA, 1969, pp. 1125–1134.